Modelling transition due to backward-facing steps using the laminar kinetic energy concept

Medina, H. J. and Early, J.

Original citation & hyperlink:
Medina, H. J. and Early, J. (2014) Modelling transition due to backward-facing steps using the laminar kinetic energy concept. European Journal of Mechanics - B/Fluids, volume 44 : 60-68
http://dx.doi.org/10.1016/j.euromechflu.2013.10.004

ISSN 0997-7546
DOI 10.1016/j.euromechflu.2013.10.004

Modelling transition due to backward-facing steps using the laminar kinetic energy concept

H. Medina[a,*], J. Early[b,1]

[a] *Faculty of Engineering and Computing, Coventry University, Engineering and Computing Building, Priory Street, Coventry - CV1 5FB.*
[b] *School of Mechanical and Aerospace Engineering, Queen's University Belfast, Stranmillis Road, Belfast - BT9 5AH.*

Abstract

Boundary layer transition estimation and modelling is essential for the design of many engineering products across many industries. In this paper, the Reynolds-Averaged Navier-Stokes are solved in conjunction with three additional transport equations to model and predict boundary layer transition. The transition model (referred to as the $k_T - k_L - \omega$ model) is based on the $k - \omega$ framework with an additional transport equation to incorporate the effects low-frequency flow oscillations in the form of a laminar kinetic energy (k_L). Firstly, a number of rectifications are made to the original $k_T - k_L - \omega$ framework in order to ensure an appropriate response to the free-stream turbulence level and to improve near wall predictions. Additionally, the model is extended to incorporate the capability to model transition due to surface irregularities in the form of backward-facing steps with maximum non-dimensional step sizes of approximately 1.5 times the local displacement thickness of the boundary layer where the irregularity is located (i.e $k/\delta^* \lessapprox 1.5$) at upstream turbulence intensities in the range $0.01 < Tu(\%) < 0.8$. A novel function is proposed to incorporate transition sensitivity due to aft-facing steps. This paper details the rationale behind the development of this new function and demonstrates its suitability for transition onset estimation on a flat plate at zero pressure gradient.

Keywords: Transition, RANS, Aft-step, Flat Plate, Tolerance, OpenFOAM

1. Introduction

The subject of boundary layer transition modelling is an area that has attracted and continues to attract significant interest. The reason for such interest is mainly due to the fact that many engineering applications involve transitional boundary layer flows. For example, within the aerospace industry there has been an increased interest in developing Unmanned-Aerial Vehicles (UAVs). Due to their relatively small size (in comparison to more traditional aircraft), UAVs operate at low-medium Reynolds numbers making their performance very susceptible to the laminar-turbulent boundary layer transition process [1, 2]. Therefore, it is of paramount importance for aerospace designers and engineers alike to have the ability to model and predict the transition process accurately. Additionally, there are many more engineering applications where the ability to accurately predict the breakdown to turbulence is essential to engineers, such as automotive, renewable energy, heat transfer and cooling, as well as maritime applications.

Historically, different approaches have been employed to model and predict boundary layer transition with various degrees of success. For example, early transition models were based on Linear Stability Theory (LST) and the e^N method [3], as well as experimental correlations [4, 5]. Whilst these methods have proven very useful and have been applied successfully to engineering design, they have a fundamental drawback. That is, they rely on experimental data in order to be calibrated and, most importantly, the calibration of these models is not universal (requiring a new calibration and additional experimental data for even the most trivial of design changes). More recently, Large Eddy Simulation (LES) and Direct Numerical Simulation (DNS) have been successfully applied to studying and predicting the boundary layer transition process [6–9]. DNS is certainly a very useful tool for the study of fluid flow phenomena. However, due to the large computational requirements for accurate predictions, DNS is still not a practical tool for most engineering applications and it is currently mostly used as a research tool at relatively low Reynolds numbers since the mesh requirement for accurate 3D channel flow DNS is proportional to $Re^{9/4}$ [10]. An alternative approach is LES where the large scales in the flow are simulated and turbulence below the inertial sub-range is modelled and assumed universal following Kolmogorov's Universal Equilibrium Theory. Excellent reviews covering the working principles of LES as well as challenges faced in its application can be found in [11, 12]. An advantage of LES (when compared to DNS) is that the smallest turbulent scales are modelled, as a result the mesh density require-

*Corresponding author. Telephone: +44 (0) 2477 65 8902
Email addresses: h.medina@coventry.ac.uk (H. Medina), j.early@qub.ac.uk (J. Early)
[1] Telephone: +44 (0) 2890 97 5663

ment is reduced, with further reductions by modelling the boundary layer near walls in wall-bounded flows [13, 14]. Since the mesh density requirement for LES also involves significant computing resources, its usage as a day-to-day engineering tool is limited. As a result, the RANS-based simulation of transitional flows continues to be an area of interest because RANS-based modelling offers a reasonable compromise between computational expense and accuracy. For this reason and due to the engineering relevance of this work a RANS-based approach was employed.

Whilst the LES and DNS approaches have been discarded in preference of a RANS-based approach due to their relative computational economy, a suitable RANS model is yet to be selected to form the basis of this work. An examination of the literature of recent RANS models developed to predict boundary layer transition shows that there are two common approaches: (i) to couple turbulent models with empirical correlations and (ii) to extend turbulence models by including additional transport equations in order to model transitional behaviour.

The first approach involves the inclusion of suitable experimental transition correlations [15, 16] which are used to determine transition initiation. The extent of the transition region is often modelled based on Dhawan and Narasimha's intermittency profile [17]. The inclusion of correlations for transition estimation within RANS-based solvers can be problematic for a number of reasons. For instance, transitional correlations often require the calculation or estimation of non-local quantities such as the distance along a surface and the momentum/displacement thickness of the boundary layer. This requirement makes their implementation more complex. Additionally, transition correlations are often deduced from experiments of simple or canonical geometries which increases the uncertainty when these correlations are applied to more complex geometries. Unless, the experimental database used to develop a given correlation is fine-tuned to particular applications, therefore, increasing the cost to develop these models.

On the other hand, the development of more general transitional models can also be accomplished by developing additional transport equations and/or by including model terms to account for the effects of transition. This could be accomplished with the use of transition estimation correlations such as the models proposed by Suzen et al. [18], Steelant et al. [19] and Menter et al [20]. However, as already mentioned, this approach can be difficult to implement. An alternative method is to develop phenomenological or physics-based models [21–23]. The development of phenomenological models [21–23] is preferable in the sense that they attempt to incorporate the physics of transition directly. However, this is a very challenging task, mainly due to the fact that the physics of transition are not yet fully understood, for example, the mechanism of receptivity of the boundary layer to external disturbances, as well as, 3-dimensional effects as a result of pressure gradients and/or complex geometries. Nonetheless, Walters and Cokljat [24] presented a phenomenological transitional model using three transport equations ($k_T - k_L - \omega$) which offers the advantage of making transition onset predictions based on local variables, therefore, facilitating its implementation. For this reason, a revised version of the model developed by Walters et al. [24] was chosen as the transition estimation framework to be extended to incorporate predictions due to surface imperfections, that is, small backward-facing steps in the range $k/\delta^* \lessapprox 1.5$.

The location of transition onset for a boundary layer is affected by variables, such as freestream turbulence levels, pressure gradients and aerodynamic surface imperfections. Aerodynamic surfaces can contain bulges, gaps, waviness and/or surface roughness. Additionally, surface imperfections can also originate due to operational conditions such as insect or ice agglomeration. The focus of this work is to extend the $k_T - k_L - \omega$ framework to add the capability of predicting transition due to backward-facing steps. This type of surface imperfection is of particular interest due to the fact that despite advances in manufacturing methods, in engineering applications, step changes in aerodynamic surfaces are often unavoidable due to the need to include access/service hatches. Additionally, including the capability to estimate transition onset combining the effects of surface imperfections and the freestream turbulence level is suited to UAV flight as different freestream turbulence intensities can be encountered depending on the UAV's operational requirements and mission.

Wang et al. [25] presented experimentally determined transition Reynolds numbers due to backward-facing steps. In this work, their experimental data is utilised to develop a correlation between the non-dimensional backward-facing step height and the corresponding (scaled) transitional Reynolds number. This correlation is used to formulate and propose a new transition threshold function at low-moderate turbulence intensities ($0.015\% < Tu < 0.8\%$) to include the effects of aft-facing steps. This transition threshold function is implemented within a proposed revision of the $k_T - k_L - \omega$ model.

2. Numerical method

2.1. Background

Walters and Cokljat [24] proposed a three-equation model, which will be referred to as the $k_T - k_L - \omega$ model, to mimic transition mechanisms and predict boundary layer transition. Depending on the free-stream turbulence intensity level, two main mechanisms leading to the transition to turbulence of the boundary layer have been observed, that is, (i) at low upstream turbulence intensities transition is initiated due to the amplification of quasi two dimensional waves known as Tollmien-Schlichting waves or T-S waves [26, 27] and (ii) at turbulence intensities approximately greater than $0.5 - 1\%$ the mechanism of T-S wave amplification is not observed, and transition occurs as a result of the breakdown or eddying of stream-wise fluctuations represented by Klebanoff modes [28]. This latter

route to transition is known as by-pass transition [29] to reflect the fact that linear amplification of T-S waves is bypassed. For succinctness, in this section only the main concepts behind this transition estimation model are briefly introduced. An excellent and detailed discussion can be found in Walters et al. [24]. A key feature of this model is that it employs the concept of laminar kinetic energy (k_L) to model low-frequency pre-transitional fluctuations. The concept of laminar kinetic energy was originally developed by Mayle and Schulz [16] in order to describe the evolution of high-amplitude stream-wise pre-transitional fluctuations that lead to by-pass transition. Whilst the physics and development of the so-called laminar kinetic energy is not fully understood, it is known that boundary layers are sensitive to specific free-stream eddy scales and that low-frequency disturbances within the boundary layer are amplified by shear mechanisms. This knowledge suggests that a phenomenological transitional model could be conceived by selecting appropriate turbulence scales and modelling the growth of low-frequency up-stream fluctuations (k_L). Also, it has been demonstrated [30, 31] that the growth of laminar kinetic energy is linear with respect to the stream-wise Reynolds number and it correlates with low-frequency normal fluctuations of the free-stream turbulence. Walters and Cokljat [24] incorporate these known features of boundary layer transition into a transport equation for k_L and extend it to incorporate a production term due to natural transition which is conveniently expressed as a function of the Reynolds number based on the local strain rate. The $k_T - k_L - \omega$ model also incorporates the concept of shear-sheltering which is used to indicate the dampening of turbulence dynamics in thin high-vorticity regions such as the pre-transitional boundary layer [32]. Essentially, the laminar regions of the boundary layer corresponded to a damped state of the turbulent solution. Therefore, the $k_T - k_L - \omega$ model uses a series of damping functions to model laminar regions, where the flow is turbulent these functions assume the value of one which returns the transport equations to their turbulent formulation ($k-\omega$ framework). Additionally, the model includes natural transition estimation by including the assumption that disturbances linked to T-S waves can be modelled using a time-scale proportional to the inverse of the vorticity. Finally, the criterion for natural boundary layer transition is a function of the ratio of the T-S time-scale to the molecular diffusion time-scale. Wang and Gaster [25] showed that transitional Reynolds numbers due to backward-facing steps correlate to N-factors obtained from linear stability theory. This suggests that natural transition due to such steps can be modelled using wave amplification/stability approaches. Therefore, since the criterion for natural boundary layer transition used by Walters and Cokljat [24] uses T-S time-scales, it is possible to develop a new functional form for the transition criterion due to backward-facing steps. The development of this function is discussed after a number of corrections are made to the original $k_T - k_L - \omega$ model in the next section.

2.2. Revised $k_T - k_L - \omega$ model

In this section the model equations are formulated for single-phase and incompressible flow without body forces. As discussed previously, the model employs the Reynolds-averaged approach to derive the momentum and continuity equations. As shown in equation (1), the eddy viscosity is modelled using the Boussinesq hypothesis which offers a linear relationship between the Reynolds stress and the strain rate tensor.

$$\rho\overline{u_i u_j} - 1/3\rho\overline{u_k u_k}\delta_i j = -2\nu_T S_{ij} \tag{1}$$

The transition sensitive model is based on the $k-\omega$ framework. In the transitional model proposed by Walters [24], the total turbulent kinetic energy, k, is modelled as $k = k_{TOTAL} = k_L + k_T$, where k_L (referred to as the laminar kinetic energy) results in a transport equation to model low-frequency pre-transitional energy fluctuations. Furthermore, k_T is also modelled using a separate transport equation to account for the magnitude of fluctuations associated with the characteristics of turbulent flow. Therefore, it is referred to as the turbulent kinetic energy. The final transport equation employs the inverse turbulent time-scale, ω, as is equivalent to the equations used in other $k-\omega$ models. These transport equations are given as:

$$\frac{Dk_T}{Dt} = P_{k_T} + R_B P + R_N A T - \omega k_T - D_T + \frac{\partial}{\partial x_j}\left[\nu + \frac{\alpha_T}{\sigma_k}\frac{\partial k_T}{\partial x_j}\right] \tag{2}$$

$$\frac{Dk_L}{Dt} = P_{k_L} - R_{BP} - R_{NAT} - D_L + \frac{\partial}{\partial x_j}\left[\nu\frac{\partial k_L}{\partial x_j}\right] \tag{3}$$

$$\begin{aligned}\frac{D\omega}{Dt} &= C_{\omega 1}\frac{\omega}{k_T}P_{k_T} + \left(\frac{C_{\omega R}}{f_W} - 1\right)\frac{\omega}{k_T}(R_{BP} + R_{NAT}) \\ &\quad - C_{\omega 2} f_W^2 \omega^2 + C_{\omega 3} f_\omega \alpha_T f_W^2 \frac{\sqrt{k_T}}{d^3} \\ &\quad + \frac{\partial}{\partial x_j}\left[\left(\nu + \frac{\alpha_T}{\sigma_\omega}\right)\frac{\partial \omega}{\partial x_j}\right]\end{aligned} \tag{4}$$

The production of laminar and turbulent kinetic energy by mean strain is modelled as:

$$P_{k_T} = \nu_{T,s} S^2 \tag{5}$$

$$P_{k_L} = \nu_{T,l} S^2 \tag{6}$$

In the production equations above, $\nu_{T,s}$ and $\nu_{T,l}$ represent the small and large-scale eddy viscosities, respectively. The latter is defined as:

$$\nu_{T,s} = f_W f_{INT} C_\mu \sqrt{k_{T,s}}\lambda_{eff} \tag{7}$$

Where the effective small-scale turbulence is given by:

$$k_{T,s} = f_{SS} f_W k_T \tag{8}$$

The kinematic wall effect is modelled using a wall limited turbulence length scale (λ_{eff}) and damping function (f_W).

$$\lambda_{eff} = min(C_\lambda d, \lambda_T) \tag{9}$$

$$\lambda_T = \frac{\sqrt{k_T}}{\omega} \tag{10}$$

$$f_W = \left(\frac{\lambda_{eff}}{\lambda_T}\right)^{3/2} \tag{11}$$

In reference to the damping function, f_W, the form included in this work differs from the original definition by Walters et al. [24] due to the inclusion of the exponent 3/2. This exponent was included in order to preserve consistency between the various terms in the equations of this model and the previous $k-\omega$ transitional formulation by Walters et. al [33].

Viscous wall effects are included using a viscous damping function (f_v) which in turn is dependent to the effective turbulence Reynolds number (Re_T).

$$f_\nu = 1 - e^{-\sqrt{Re_T}/A_\nu} \tag{12}$$

$$Re_T = (f_W^2 k_T)/\nu\omega \tag{13}$$

The shear-sheltering effect is included through the damping functions below.

$$f_{SS} = e^{-(C_{ss}\nu\Omega/k_T)^2} \tag{14}$$

In order to satisfy the realisability constraint suggested by Shih et al. [34], the turbulent viscosity coefficient takes the form:

$$C_\mu = \frac{1}{A_0 + A_s\left(\frac{S}{\omega}\right)} \tag{15}$$

Intermittency effects on the production of turbulence are included through the intermittency damping function (f_{INT}). The expression shown in equation (16) is a correction to the original paper [24] where the laminar kinetic energy (k_L) was included instead of the turbulent kinetic energy (k_T).

$$f_{INT} = min\left(\frac{k_T}{C_{INT} k_{TOTAL}}, 1\right) \tag{16}$$

The large-scale contribution to the total turbulent kinetic energy is defined as:

$$k_{T,l} = k_T - k_{T,s} \tag{17}$$

The production of laminar kinetic energy is modelled as the product of the large-scale eddy viscosity times the square of the magnitude of the mean strain. The model for the large-scale eddy viscosity is shown in equation (19).

$$P_{k_L} = \nu_{T,l} S^2 \tag{18}$$

$$\begin{aligned}\nu_{T,l} &= min\Bigg\{\left[f_{\tau,l} C_{l1}\left(\frac{\Omega\lambda_{eff}^2}{\nu}\right)\sqrt{k_{T,l}}\lambda_{eff}\right. \\ &\left. +\beta_{TS} C_{l2} Re_\Omega d^2\Omega\right], \left[\frac{k_L + k_{T,l}}{2S}\right]\Bigg\}\end{aligned} \tag{19}$$

Where,

$$Re_\Omega = \frac{d^2\Omega}{\nu} \tag{20}$$

$$\beta_{TS} = 1 - e^{\left[\frac{max(Re_\Omega - C_{TS,crit},0)^2}{A_{TS}}\right]} \tag{21}$$

$$f_{\tau,l} = 1 - e^{-\left(C_{\tau,l}\frac{k_{T,l}}{\lambda_{eff}^2\Omega^2}\right)} \tag{22}$$

The anisotropic dissipation terms which appear in the transport equations for k_L and k_T are modelled as shown in equations (23) and (24). This form is exactly as proposed in Walters et al. [24]. However, in the previous models [23, 33] the anisotropic dissipation terms include a multiplication by a factor of 2. The form shown below was used in the current work and yielded excellent results.

$$D_T = \nu\frac{\partial\sqrt{k_T}}{\partial x_j}\frac{\partial\sqrt{k_T}}{\partial x_j} \tag{23}$$

$$D_L = \nu\frac{\partial\sqrt{k_L}}{\partial x_j}\frac{\partial\sqrt{k_L}}{\partial x_j} \tag{24}$$

The effective diffusivity (α_T) which appears on the transport equations for both the turbulent kinetic energy and the inverse turbulence time-scale is defined as:

$$\alpha_T = f_\nu C_{\mu,std}\sqrt{k_{T,s}}\lambda_{eff} \tag{25}$$

The kinematic damping function (f_ω) is included in the transport equation for the inverse turbulence time-scale in order to control production of the boundary layer wake region.

$$f_\omega = 1 - e^{-0.41\left(\frac{\lambda_{eff}}{\lambda_T}\right)^4} \tag{26}$$

The expressions that follow are included in order to model the transition process where, conceptually, energy is transferred from the laminar kinetic energy to the turbulent kinetic energy. The term R_{BP} is used to model bypass transition mechanisms and R_{NAT} is used to model the natural breakdown of linear instabilities in the form of TS-waves into turbulence. For succinctness, a detailed explanation of the mechanisms by which these expressions control transition is not included in this paper. However,

an excellent explanation of the rationale for the development of these expressions is provided by Walters et al. [23, 24, 33].

$$R_{BP} = C_R \beta_{BP} k_L \omega / f_W \tag{27}$$

$$R_{NAT} = C_{R,NAT} \beta_{NAT} k_L \Omega \tag{28}$$

In equation (27), β_{BP} acts as a threshold function to initiate the transition from laminar to turbulent flow when by-pass transition is considered. The threshold function is controlled by the inclusion of the limiting function ϕ_{BP}. Notice that the form of this limiting function is not the same as that originally included in Walters et al. [24], instead the function takes the form presented in Walters et al. [33]. This modification was made to the model because the original form led to a non-physical response for the estimated transition locations at low turbulence intensities ($Tu_\infty < 0.9\%$). In summary, as the free-stream turbulence intensity was increased, the onset of transition shifted downstream. However, by reverting to the form shown in equation (30), the model responded correctly to changes in the free-stream turbulence level.

$$\beta_{BP} = 1 - e^{-\left(\frac{\phi_{BP}}{A_{BP}}\right)} \tag{29}$$

$$\phi_{BP} = max\left[\left(\frac{\sqrt{k_T}d}{\nu} - C_{BP,crit}\right), 0\right] \tag{30}$$

The remaining terms are included in the model in order to control the natural transition mechanism. Again, a threshold function (β_{NAT}) is included to initiate transition to turbulence due to the breakdown of linear instabilities. This process is controlled by the limiting function ϕ_{NAT} which uses the Reynolds number based on magnitude of the mean rotation rate tensor (Re_Ω). When Re_Ω is larger than a critical value ($C_{NAT,crit}/f_{NAT,crit}$) the production term R_{NAT} starts contributing to the production of turbulent kinetic energy (k_T).

$$\beta_{NAT} = 1 - e^{-\left(\frac{\phi_{NAT}}{A_{NAT}}\right)} \tag{31}$$

$$\phi_{NAT} = max\left[\left(Re_\Omega - \frac{C_{NAT,crit}}{f_{NAT,crit}}\right), 0\right] \tag{32}$$

$$f_{NAT,crit} = 1 - e^{-\left(C_{NC}\frac{\sqrt{k_L}d}{\nu}\right)} \tag{33}$$

In this work, the initiation of natural transition as controlled by β_{NAT} is extended to include predictions of natural transition due to backward-facing steps. This is accomplished by a proposed modification of the limiting function ϕ_{NAT}. The development of a new form for this function capable of estimating transition onset due to backward-facing steps will be explored in section 3.2. Finally, table 1 presents the values of the various model coefficients used in this work. Notice that the coefficient $C_{BP,crit}$ assumes the value of 12 based on the previously suggested value for this coefficient [33].

2.3. Numerical setup

The model equations described section 2.2 were implemented in OpenFOAM 2.1.1 by modifying the standard implementation of the Walters et al. [24] model included with this release in order to incorporate the changes to the original model suggested in section 2.2. Also, additional modifications were included in order to debug the model and improve stability. The Reynolds-averaged Navier-Stokes equations (continuity and momentum) and three additional transport equations (k_T, k_L and ω) were solved using the Semi-Implicit Method for Pressure Linked Equations (SIMPLE) algorithm implemented and included in the standard release of OpenFOAM 2.1.1. The SIMPLE algorithm implementation in OpenFOAM also allows applying relaxation factors to each model variable. The default values were used for all the simulations presented herein. That is, a relaxation factor of 0.3 was set for the pressure field, and a value of 0.7 for all the other fields. Finally, all simulations were allowed to converge until the final values of the dimensionless residual for all equations reached values of at least 10^{-8} or less.

OpenFOAM offers immense flexibility to perform the discretisation of the model equations, and end-users have the freedom to select discretisation schemes for each term that appears on the set of equations to be solved. In the simulations presented in this work the various terms in the model equations were discretised using the standard finite volume discretisation of Gaussian integration. The gradient terms require the interpolation of values between cell centres to face centres, this was achieved using linear interpolation. For Laplacian terms, diffusion coefficients were discretised using linear interpolation and surface normal gradients were discretised using a corrected scheme which offers second order accuracy. Finally, divergence schemes were discretised using a blended linear upwind scheme offering both first and second order accuracy. This scheme was selected because it provides a suitable compromise between stability and accuracy. The various transition estimations for the flow over a flat plate at zero-pressure gradient were carried out in the two-dimensional domain shown in figure 1, where the inlet boundary is located $0.8m$ upstream from the leading edge of the flat plate. The domain also stretches $0.8m$ measured vertically upwards (y-direction) from the leading edge. At the outlet, the domain has a height of $0.794m$ due to the thickness of the plate. The plate has a length of $4m$ and a half-thickness equal to $0.006m$. Also, in order to allow the formation of a stagnation point, an elliptical leading edge profile with a major-to-minor axis ratio equal to 6 was used. The main features of the geometry and mesh near the leading edge is shown in figure 2. A hexahedral mesh containing $82,200$ cells distributed in a $600x137$ grid was used. The optimum density of the grid was determined by sequentially doubling the number of nodes in the x and y directions and selecting the mesh with a cell density for which a further increase in mesh density led to negligible differences in results. Also, since a low-Reynolds model is to be used, the

$A_0 = 4.04$	$A_S = 2.12$	$A_\nu = 6.75$	$A_{BP} = 0.6$	$A_{NAT} = 200$
$A_{TS} = 200$	$C_{BP,crit} = 12$	$C_{NC} = 0.1$	$C_{INT} = 0.75$	$C_{TS,crit} = 1000$
$C_{R,NAT} = 0.02$	$C_{l1} = 3.4x10^{-6}$	$C_{l2} = 1.0x10^{-10}$	$C_R = 0.12$	$C_{\alpha,0} = 0.035$
$C_{SS} = 1.5$	$C_{\tau,l} = 4360$	$C_{\omega 1} = 0.44$	$C_{\omega 2} = 0.92$	$C_{\omega 3} = 0.30$
$C_{\omega R} = 1.5$	$C_\lambda = 2.495$	$C_{\mu,std} = 0.09$	$\sigma_k = 1$	$\sigma_\omega = 1.17$

Table 1: $k_T - k_L - \omega$ model coefficients

mesh was constructed such that the cell-centred y^+ value of the cells closest to the surface of the plate is 1 or less for all the conditions tested. The simulations were performed employing the boundary conditions suggested by Walter et al. [24]. The velocity and turbulent quantities (k_T, ω) were specified using a Dirichlet boundary condition at the inlet. The laminar kinetic energy (k_L) was given a value equal to zero at the inlet which is a reasonable estimate provided the inlet is sufficiently far from the plate. The pressure was assigned a value of zero at the outlet boundary (because the flow is incompressible only relative pressure differences are needed). The pressure was given a zero-gradient Newmann boundary condition at all other boundaries. A symmetry boundary condition was imposed on the boundaries parallel to the plate as shown in figure 1. At the wall, and due to the non-slip condition, the velocity is set to zero. Since the velocity is equal to zero, the kinetic energy at the wall must also reduce to zero. Therefore, turbulent and laminar kinetic energies are set to zero at the plate wall. The model used in this work differs from other $k-\omega$ models due to the required boundary condition that must be given to the turbulent inverse time-scale at walls, requiring a zero-gradient Neumann boundary condition. The model was also tested by setting ω equal to zero at the wall. Remarkably, the model yields almost identical results regardless of which condition is chosen. However, setting ω equal to zero as a boundary condition at the wall proved to be less stable. Interestingly, Walters et al. [24] did not observe or reported this behaviour. This could be due to the fact that a different algorithm was used to solve the differential equations. Finally, the implementation of the model in OpenFOAM also requires the user to provide suitable boundary conditions for the eddy viscosity (ν_T). This is the means by which wall functions are controlled in OpenFOAM. Since wall functions are not required for this transitional model, the "calculated" boundary condition was selected for all boundaries with the exception of the symmetry boundaries which were assigned a symmetry condition. The symmetry boundaries were employed because they help improve the stability of the calculations. The use of a symmetry boundary at the patch directly upstream from the leading edge is particularly effective in stabilising calculations because it allows the development of a stagnation point at the leading edge of the flat plate. A summary of the boundary conditions used is given in table 2.

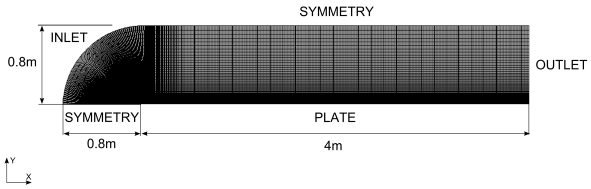

Figure 1: Schematic of the computational domain and boundaries

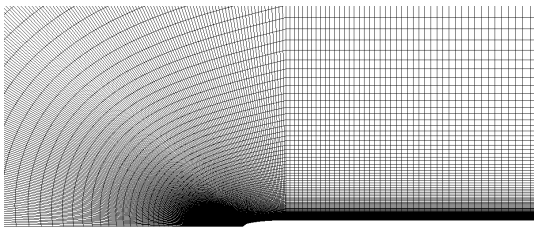

Figure 2: Close up of the numerical grid near the leading edge of the flat plate

3. Results and discussion

3.1. Revised $k_T - k_L - \omega$ model: Flat plate test cases

Prior to the extension of the model to incorporate transition estimation capabilities due to backward-facing steps, the revised $k_T - k_L - \omega$ framework introduced previously will be validated using experimental results at low-moderate turbulence intensities ($Tu_\infty \leq 0.8\%$). The inlet free-stream conditions used for these simulations are summarised in table 3. For simplicity, the model is validated based on its ability to predict transition onset over a flat plate at zero pressure gradient. The model was tested (using the spatial and numerical discretisation detailed in section 2.3) at two different turbulence intensity levels ($Tu = 0.035\%$ and $Tu = 0.8\%$) and compared to the experimental results of Wang et al. [22] and Feiereisen et al. [35].

Figure 3 shows the development of the skin friction coefficient along the length of the plate as a function of the local Reynolds number Re_x. This figure shows that the model modifications proposed in the previous section lead to a model capable of offering reasonable predictions of boundary layer transition onset, at least for a simple geometry such as the flow over a flat plate at zero pressure gradient. The experimental transitional Reynolds number (based on the streamwise location where the skin friction is a minimum) for $Tu = 0.03\%$ and $Tu = 0.7\%$ is estimated at $0.8x10^5$ and $2.5x10^6$, respectively. The revised

	U (m/s)	p/ρ (m^2/s^2)	k_L (m^2/s^2)	k_T (m^2/s^2)	ω (s^{-1})	ν_T
Inlet	$U = U_\infty$	$\frac{\partial p/\rho}{\partial x_i} = 0$	$k_L = 0$	$\frac{3}{2}(TuU_\infty)^2$	$\frac{C_{\mu,std}k_T}{\nu_R \nu}$	calculated
Outlet	$\frac{\partial U}{\partial x_i} = 0$	$\frac{p}{\rho} = 0$	$\frac{\partial k_L}{\partial x_i} = 0$	$\frac{\partial k_T}{\partial x_i} = 0$	$\frac{\partial \omega}{\partial x_i} = 0$	
Plate	$U_i = 0$	$\frac{\partial p/\rho}{\partial x_i} = 0$	$k_L = 0$	$k_T = 0$	$\frac{\partial \omega}{\partial x_i} = 0$	
Symmetry	symmetryPlane					

Table 2: Generic summary of boundary conditions

Case	$Tu_\infty(\%)$	$U_\infty(m/s)$	ν_R	$k_L(m^2/s^2)$	$k_T(m^2/s^2)$	$\omega(s^{-1})$
Tu0p035R04	0.035	12	4	0	$2.646x10^{-5}$	$3.969x10^{-2}$
Tu0p800R04	0.800	10.5	4	0	$10.584x10^{-3}$	15.876

Table 3: Inlet conditions used for the flat plate test cases

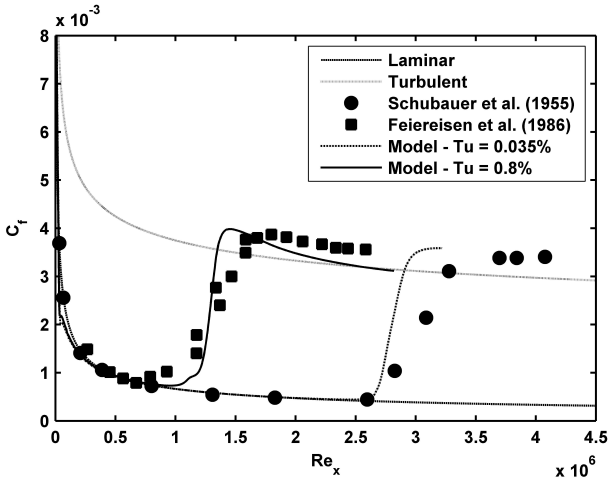

Figure 3: Comparison between model transition predictions at two turbulence intensity levels ($Tu = 0.035\%$ and $Tu = 0.8\%$) and the experimental results of Schubauer et al. [36] (extracted from Wang et al. [22]) and Feiereisen et al. [35]

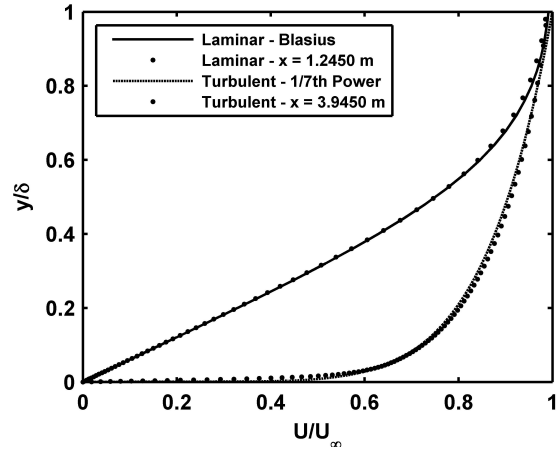

Figure 4: Laminar (Blasius) and turbulent ($1/7^{th}$ power) velocity profiles comparison against predicted velocity profiles.

transition model, for $Tu = 0.035\%$ and $Tu = 0.8\%$ (at the inlet boundary), produces estimates of the transitional Reynolds number of $0.9x10^5$ and $2.6x10^6$, respectively. It is worthwhile to highlight that figure 3 also demonstrates that the model exhibits an appropriate physical response to changes in free-stream turbulence and transition initiation shifts upstream with increasing the free-stream turbulence intensity.

Additionally, laminar and turbulent boundary layer velocity profiles are also shown in figure 4. This figure shows that there is an excellent agreement between the theoretical and calculated boundary layer velocity profiles. Whilst a more detailed validation of the model is still required if it is to be used with complex geometries, for the current investigation is was considered sufficient to establish that (i) the model responds physically to the location of the calculated transition onset location as a result of free-stream turbulence intensities and (ii) the model can predict both laminar and turbulent boundary layer profiles over a flat plate at zero pressure gradient.

3.2. Backward-facing step: concept and implementation

This section will detail the rationale and methodology used in order to incorporate into the $k_T - k_L - \omega$ framework described previously the capability to predict boundary layer transition locations due to a single backward-facing step surface irregularity for free-stream turbulence intensities in the range $0.01 - 0.8\%$. This range is selected because it falls within the observable range for natural transition and is lower than the 1% level typically linked to by-pass transition initiation [37]. Also, for turbulence intensities approximately less than 0.9%, transition initiation for the $k_T - k_L - \omega$ model is dominated by the natural transition production term shown in equation (28). In turn, transition initiation is controlled by the threshold function $\beta_{NAT,crit}$ which also depends on the function ϕ_{NAT} to regulate the behaviour of the damping function by evaluating the difference:

$$Re_\Omega - C_{NAT,crit}/f_{NAT,crit} \tag{34}$$

The proposed extension of the $k_T - k_L - \omega$ framework to incorporate the prediction of boundary layer transition due to surface steps is based on developing a new form

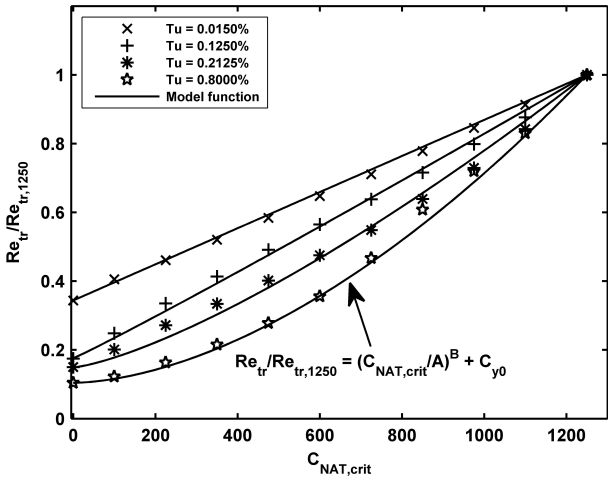

Figure 5: Effect of CNAT,crit on the estimated transition onset locations

for the natural transition threshold function β_{NAT} based on the experimental data reported by Wang and Gaster [25] who also demonstrated that the non-dimensional step height (k/δ^*) can be correlated to the N-factor resulting from the e^N method. This link to linear stability theory is encouraging since it implicitly suggests that the location of transition can be associated to TS-wave development. In the current work this response will be incorporated through a functional form for the coefficient $C_{NAT,crit}$. Firstly, the response of the model to changes in the values of C_{NAT} was investigated for at four different free-stream turbulence intensity levels (figure 5). The transitional Reynolds number, Re_{tr}, was determined by finding the stream-wise Reynolds number, Re_x, for which the value of the skin friction coefficient is a minimum. Notice that the transitional Reynolds number in figure 5 is scaled with respect to the estimated transitional Reynolds number when $C_{NAT,crit} = 1250$ which has been labelled $Re_{tr,1250}$ for convenience. Figure 5 shows that the response at low turbulence intensities ($Tu < 0.125\%$) is linear and, for $Tu > 0.2\%$, there is a modest deviation from linearity. For simplicity, the response of the model was approximated using an exponential function and $Tu = 0.8\%$ is set as the upper limit for its applicability. When using an exponential function the maximum discrepancy between the simulation results for $Re_{tr}/Re_{tr,1250}$ and the exponential fit is less than 12%.

Based on figure 5, the scaled transitional Reynolds number (labelled $Re_{tr}/Re_{tr,1250}$) will assume an exponential relationship with the general form given in equation (35). From this figure, it is straight forward to determine that the value of the coefficient, C_{y0}, represents the value of the scaled transitional Reynolds number for $C_{NAT,crit} = 0$ at each turbulence intensity. Additionally, the remaining coefficients can be determined using the expressions shown in equations (36) and (37). The coefficient A serves the purpose of scaling the model function whilst the coefficient B serves to control its non-linearity. However, both of these coefficients depend on the value of C_{y0} which is a function of the free-stream turbulence level defined as $Tu = 100(u'_{rms}/U_\infty)$. Therefore, it is paramount to find a suitable correlation between the free-stream turbulence level and the coefficient C_{y0}.

$$Re_{tr}/Re_{tr,1250} = (C_{NAT,crit}/A)^B + C_{y0} \tag{35}$$

$$A = 1250/(1 - C_{y0})^{1/B} \tag{36}$$

$$B = 1 + \left[1 - (0.95 - 0.25Tu)^{9/2}\right] f_{LOW} \tag{37}$$

The damping function f_{LOW} has been included in order to preserve linearity of the resulting function at low turbulence intensities and it has the form shown in equation (38).

$$f_{LOW} = 1 - e^{-5000Tu^5} \tag{38}$$

The variation of the coefficient C_{y0} with respect to the free-stream turbulence intensity is shown in figure 6 which shows that this coefficient exhibits an exponential decline with respect to the turbulence intensity. This relationship is not surprising as previous investigations [15, 16, 38] on boundary layer transition have shown a reduction in transitional Reynolds numbers as the free-stream turbulence level is increased e.g. Mayle [16] proposes a correlation for estimating the transitional Reynolds number over a flat plate as a function of the free-stream turbulence intensity which exhibits an exponential decline proportional to 5/8 (a similar rationale can be used to explain the origin of the exponent used in equation (43)). Consequently, the coefficient C_{y0} can be correlated to the turbulence intensity using the expression:

$$C_{y0} = \frac{Re_{tr,0}}{Re_{tr,1250}} = aTu^b + c \tag{39}$$

Where,

$$a = 0.05075 \tag{40}$$

$$b = -0.4424 \tag{41}$$

$$c = 0.0482 \tag{42}$$

The values of the coefficients shown in equations (40), (41) and (42) correspond to a 99% confidence level fit (see figure 6). Additionally, the sensitivity of the coefficients to the turbulence intensity is such that, for the function shown in (39) to offer fits within a 95% confidence level, the coefficients a, b and c can assume values that fall within the ranges $(-0.00415, 0.1056)$, $(-0.6502, -0.2346)$ and $(-0.02444, 0.1208)$, respectively. In summary, using equations (36) to (42) help defining equation (35) which provides an expression of the scaled transitional Reynolds

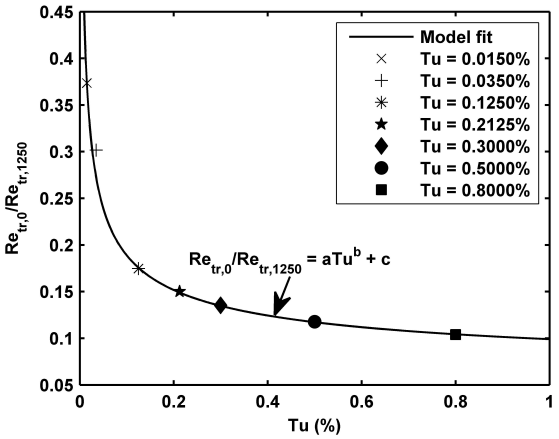

Figure 6: Relationship between C_{y0} and the free-stream turbulence intensity

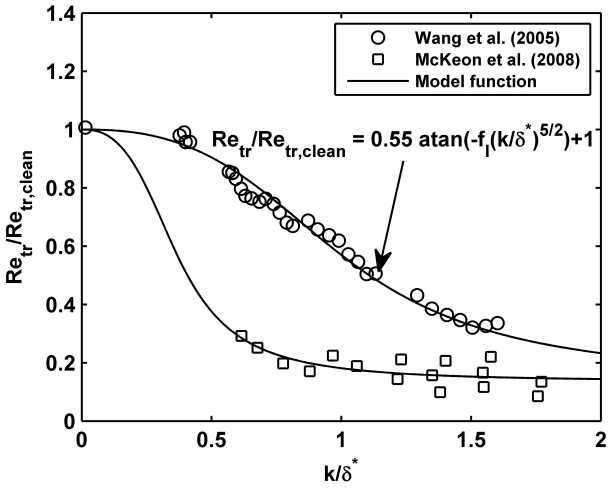

Figure 7: Scaled model function fit (equation (43)) at two different free-stream turbulence levels; $Tu \approx 0.01\%$ (Wang et al. [25]) and $Tu \approx 0.2$ (McKeon et al. [39] and Drake et al. [40])

number ($Re_{tr}/Re_{tr,1250}$) as a function of the free-stream turbulence intensity (expressed as a percentage) and the coefficient $C_{NAT,crit}$.

The next step is to find a suitable model for representing the experimental data [25, 39] correlating the dimensionless height (k/δ^*) of a single backward-facing step to the transitional Reynolds number, Re_{tr}. The proposed method to accomplish this task is to scale the experimental values of Re_{tr} using the transitional Reynolds number measured on the clean plate ($Re_{tr,clean}$). This scaling approach is suggested as a means to include into the model a sense of self-calibration. It is proposed to model the experimental data (after scaling) using the trigonometric inverse tangent function such that the expression shown in equation (43) becomes the proposed model function:

$$\frac{Re_{tr}}{Re_{tr,clean}} = C_1 atan\left[-f_I\left(\frac{k}{\delta*}\right)^{\frac{5}{2}}\right] + 1 \qquad (43)$$

Where,

$$C_1 = 0.55 \qquad (44)$$

In an attempt to also include the effects of varying the free-stream turbulence intensity level, the coefficient f_I takes the functional form:

$$f_I = 100Tu \qquad (45)$$

Figure 7 shows the proposed model function (equation (43)) plotted against the experimental data presented by Wang et al. [25] and McKeon et al. [39] in order to demonstrate its suitability. It is worth highlighting that due to the limited experimental data available, as well as the scatter found in the experimental data, the proposed model function can be used with relative confidence for $k/\delta^* > 0.5$. However, additional and detailed experimental measurements are required in order to refine this model function and to increase confidence in results for $k/\delta^* < 0.5$.

The final step to include the effect of backward-facing steps into the $k_T - k_L - \omega$ model is to establish a functional form for the original coefficient $C_{NAT,crit}$. This has been accomplished by equating equations (35) and (43), then solving for $C_{NAT,crit}$.

$$C_{NAT,crit} = A\left\{C_1 atan\left[-f_I\left(\frac{k}{\delta*}\right)^{5/2}\right] + 1 - C_{y0}\right\}^{1/B} \qquad (46)$$

The resulting model function is shown in equation (46). At present, it is only applicable for $C_{NAT,crit} \geq 0$ which has been deemed appropriate due to the scatter in experimental results as the non-dimensional step size (k/δ^*) is increased. Additionally, the current limit of applicability (i.e. $C_{NAT,crit} = 0$) is relevant for many engineering applications.

3.3. Backward-facing steps: Test cases

The methodology described in the previous section will be tested using the experimental data for backward-facing steps presented by Drake et al. [40]. The benchmark test cases consist of a single aft-facing step surface irregularity placed on a flat plate at zero pressure gradient. The numerical set up and mesh are presented in section 2.3. The inlet conditions were adjusted to more closely match the experimental configuration. A summary of the inlet conditions can be found in table 4. For the benefit of CFD practitioners, it is worthwhile to highlight that the inlet turbulence intensity reported in the experiments is approximately 0.2%. However, the turbulence intensity at the inlet was set at the higher value of 0.2125% in order to ensure that the turbulence level decays to a value of approximately 0.2% at the leading edge. During the course of this investigation it was found that the $k_T - k_L - \omega$ model is sensitive to the turbulence level given to the inlet

Case	$Tu_\infty(\%)$	$U_\infty(m/s)$	ν_R	$k_L(m^2/s^2)$	$k_T(m^2/s^2)$	$\omega(s^{-1})$
Tu0p2125R4KD118	0.2125	10.5	4	0	$7.47x10^{-4}$	1.1205
Tu0p2125R4KD096	0.2125	10.5	4	0	$7.47x10^{-4}$	1.1205

Table 4: Inlet conditions used for the flat plate test cases with an aft-facing surface step

boundary. Therefore, it is recommended to ensure that the desired turbulence level is reached at the leading edge and not just assigned to the inlet boundary.

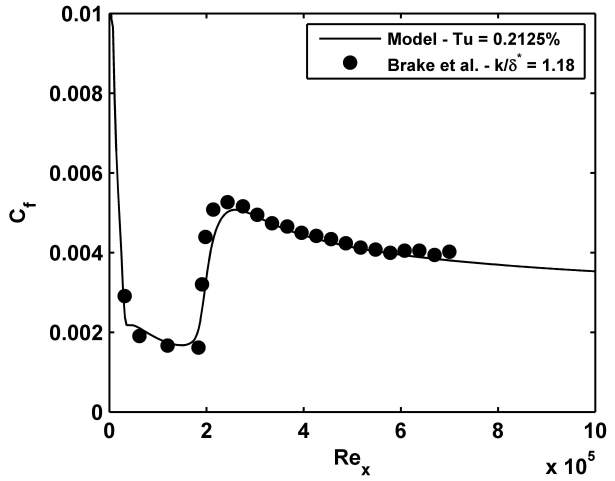

(a) $k/\delta^* = 0.96$

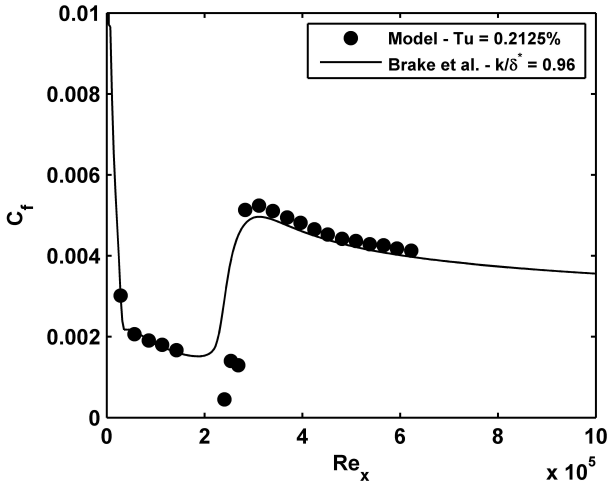

(b) $k/\delta^* = 1.18$

Figure 8: Comparison between predicted and experimental skin friction distributions

Figure 8 compares the predicted skin friction distribution over the flat plate with the experimental results of Drake et al. [40] for a non-dimensional backward-facing step height of $k/\delta^* = 0.96$. Furthermore, in order to test the proposed model close to its limit of applicability, it was also benchmarked against an additional experimental configuration. Figure 8 shows the performance of the model for $k/\delta^* = 1.18$. Figures 8a and 8b demonstrate that the proposed approach to model transition due to single aft-facing surface irregularities within the $k_T - k_L - \omega$ framework yields excellent results.

4. Conclusions

Whilst it is extremely difficult to fully capture the physics of transition by solving the Reynolds-Averaged Navier-Stokes, the $k_T - k_L - \omega$ framework has been shown to be able to predict boundary layer transition on the canonical configuration of a flat plate at zero-pressure gradient with reasonable accuracy, suggesting that this model has the potential to become an effective engineering tool to aiding aerodynamic design. Additionally, this paper presented the development of a novel function to model the effects of aft-facing steps on the transition to turbulence of the boundary layer for steps heights of up to 1.5 times the displacement thickness (i.e k/δ^*) at moderate turbulence intensities ($0.01 < Tu(\%) < 0.8$). It was found that the new function, when incorporated into the revised $k_T - k_L - \omega$ model, responded physically to the free-stream turbulence level and was able to produce reasonable predictions of the location of transition onset based on the surface skin friction over a flat plate at zero-pressure gradient. Nonetheless, there is potential to extend the basic principles presented in the work to incorporate additional surface irregularities, and to extend the applicability of this model to larger values of k/δ^* and free-stream turbulence intensity in order to predict the effects that manufacturing defects can have, not only when the flow is within the range of turbulence intensities typical of natural transition, but also when turbulence intensity levels are increased to those leading to by-pass transition. However, there is a general need for further experimental data before this vision could be fulfilled. In particular, there is a need for high quality experimental data at lower values of k/δ^*, but also, for a wider range of free-stream turbulence intensities, especially for $Tu > 0.2\%$.

References

[1] W. Shyy, Y. Lian, J. Tang, V. Dragos, H. Liu, Aerodynamics of Low Reynolds Number Flyers, Cambridge University Press, 2007.

[2] S. Serdar Genç, I. Karasu, H. Hakan Açikel, M. Tuğrul Akpolat, Low Reynolds Number Flows and Transition, Low Reynolds Number Aerodynamics and Transition, Dr. Mustafa Serdar Genç (Ed.), InTech, 2012.

[3] J. Van Ingen, The e^n method for transition prediction. historical review of work at tu delft, 38th AIAA Fluid Dynamics Conference and Exhibit.

[4] F. Hachem, M. W. Johnson, Boundary layer transition correlation for concave surfaces, American Society of Mechanical Engineers (1990) GT222 7p – GT222 7p.

[5] J. Masad, M. Malik, Transition correlation in subsonic flow over a flat plate, AIAA journal 31 (10) (1993) 1953 – 1955.
[6] L. Chen, X. Liu, M. Oliveira, C. Liu, Dns for late stage structure of flow transition on a flat-plate boundary layer, 48th AIAA Aerospace Sciences Meeting Including the New Horizons Forum and Aerospace Exposition.
[7] D. Meyer, U. Rist, S. Wagner, Dns of the generation of secondary vortices in a transitional boundary layer, Advances in Turbulence VII. Proceedings of the Seventh European Turbulence Conference (1998) 97 – 100.
[8] C. Liu, P. Lu, Dns study on physics of late boundary layer transition, 50th AIAA Aerospace Sciences Meeting Including the New Horizons Forum and Aerospace Exposition.
[9] P. Lu, C. Liu, Dns study on mechanism of small length scale generation in late boundary layer transition, Physica D 241 (1) (2012) 11 – 24.
[10] D. C. Wilcox, Turbulence Modeling for CFD, DCW Industries Inc., La Cañada, CA, 1993.
[11] U. Piomelli, Large-eddy simulation: achievements and challenges, Progress in Aerospace Sciences 35 (4) (1999) 335 – 362.
[12] R. Bouffanais, Advances and challenges of applied large-eddy simulation, Computers and Fluids 39 (5) (2010) 735 – 738.
[13] D. R. Chapman, Computational aerodynamics development and outlook., AIAA journal 17 (12) (1978) 1293 – 1313.
[14] H. Choi, P. Moin, Grid-point requirements for large eddy simulation: Chapman's estimates revisited, Physics of Fluids 24 (1).
[15] B. Abu-Ghannam, R. Shaw, Natural transition of boundary layers - the effects of turbulence, pressure gradient, and flow history., Journal of Mechanical Engineering Science 22 (5) (1980) 213 – 228.
[16] R. E. Mayle, Role of laminar-turbulent transition in gas turbine engines, American Society of Mechanical Engineers 113 (4) (1991) 509 – 536.
[17] S. Dhawan, R. Narasimha, Some properties of boundary layer flow during the transition from laminar to turbulent motion, Journal of Fluid Mechanics 3 (1958) 418–436.
[18] Y. Suzen, P. Huang, Modeling of flow transition using an intermittency transport equation, Transactions of the ASME. Journal of Fluids Engineering 122 (2) (2000) 273 – 84.
[19] J. Steelant, E. Dick, Modeling of laminar-turbulent transition for high freestream turbulence, Transactions of the ASME. Journal of Fluids Engineering 123 (1) (2001) 22 – 30.
[20] F. Menter, R. Langtry, S. Likki, Y. Suzen, P. Huang, S. Volker, A correlation-based transition model using local variables-part i: model formulation, Transactions of the ASME. The Journal of Turbomachinery 128 (3) (2006) 413 – 22.
[21] J. Edwards, C. Roy, F. Blottner, H. Hassan, Development of a one-equation transition/turbulence model, AIAA Journal 39 (9) (2001) 1691 – 8.
[22] C. Wang, B. Perot, Prediction of turbulent transition in boundary layers using the turbulent potential model, Journal of Turbulence 3 (2002) 1 – 15.
[23] D. Walters, J. Leylek, A new model for boundary layer transition using a single-point rans approach, Transactions of the ASME. The Journal of Turbomachinery 126 (1) (2004) 193 – 202.
[24] D. Walters, D. Cokljat, A three-equation eddy-viscosity model for reynolds-averaged navier-stokes simulations of transitional flow, Journal of Fluids Engineering 130 (12) (2008) 1–14.
[25] Y. Wang, M. Gaster, Effect of surface steps on boundary layer transition, Experiments in Fluids 39 (4) (2005) 679 – 86.
[26] H. Schlichting, Boundary layer theory: Seventh edition., McGraw-Hill, 1979.
[27] P. Baines, S. Majumdar, H. Mitsudera, The mechanics of the tollmien-schlichting wave, Journal of Fluid Mechanics 312 (1996) 107–124.
[28] P. Klebanoff, Effects of free-stream turbulence on a laminar boundary layer, Bull. Am. Phys. Soc. 10 (1971) 1323.
[29] M. V. Morkovin, The many faces of transition, Viscous Drag Reduction, Plenum Press, New York, 1969.
[30] R. Volino, T. Simon, Boundary layer transition under high free stream turbulence and strong acceleration conditions. 2. turbulent transport results, Transactions of the ASME. Journal of Heat Transfer 119 (3) (1997) 427 – 32.
[31] S. Leib, D. Wundrow, M. Goldstein, Effect of free-stream turbulence and other vortical disturbances on a laminar boundary layer, Journal of Fluid Mechanics 380 (1999) 169 – 203.
[32] R. Jacobs, P. Durbin, Shear sheltering and the continuous spectrum of the orr-sommerfeld equation, Physics of Fluids 10 (8) (1998) 2006 – 11.
[33] D. Walters, J. Leylek, Computational fluid dynamics study of wake-induced transition on a compressor-like flat plate, Transactions of the ASME. The Journal of Turbomachinery 127 (1) (2005) 52 – 63.
[34] T. H. Shih, W. W. Liou, A. Shabbir, Z. Yang, J. Zhu, New k-eddy viscosity model for high reynolds number turbulent flows, Computers and Fluids 24 (3) (1995) 227 – 238.
[35] W. Feiereisen, M. Acharya, Modeling of transition and surface roughness effects in boundary-layer flows, AIAA Journal 24 (10) (1986) 1642 – 9.
[36] G. B. Schubauer, P. S. Klebanoff, Contribution to the mechanism of boundary-layer transition, Tech. Rep. TN-3489, NACA (1955).
[37] M. Matsubara, P. Alfredsson, Disturbance growth in boundary layers subjected to free-stream turbulence, Journal of Fluid Mechanics 430 (2001) 149 – 68.
[38] A. Fasihfar, M. W. Johnson, An improved boundary layer transition correlation, 37th ASME International Gas Turbine and Aeroengine Congress and Exposition.
[39] B. Mckeon, A. Bender, R. Westphal, A. Drake, Transition in incompressible boundary layers with two-dimensional excrescences, 46th AIAA Aerospace Sciences Meeting and Exhibit.
[40] A. Drake, A. Bender, W. Solomon, A. Vavra, Prediction of manufacturing tolerances for laminar flow, Tech. Rep. AFRL-VA-WP-TR-2005-3060, Airforce Research Laboratory (June 2005).

Vitae

Humberto Medina

Humberto Medina is a senior lecturer at Coventry University. He obtained his undergraduate and doctoral degrees in Aerospace Engineering from the Queen's University of Belfast. His research interests include experimental and numerical fluid mechanics, applied aerodynamics and their integration into engineering design.

Juliana Early

Juliana Early is a lecturer at the School of Mechanical and Aerospace Engineering, Queens University Belfast. She received her undergraduate degree in Aerospace Engineering from the University of Glasgow in 2000, and PhD in Aerodynamics in 2006. Her research interests include applied aerodynamic design methods, aerodynamic optimisation techniques and engineering systems design.